Song *et al. Herit Sci* (2021) 9:12
https://doi.org/10.1186/s40494-021-00488-2

Heritage Science

RESEARCH ARTICLE Open Access

Craftsmanship and materials: painted Bodhisattva sculptures in the Fengguo Temple dated to the year 1020 in Yi County, Northeast China

Jiahang Song[1], Wei Xiang[1], Shaojun Yan[1*], Weiqiang Zhou[2] and Linyan Ma[3]

Abstract

As a royal temple, the Fengguo Temple has profound historical, artistic, scientific and social values. With a thousand-year history, it is one of the three existing temples of the Liao Dynasty in China. Now there remains the Main Hall with delicate wall paintings and vivid painted sculptures. The research subject of this paper is the painted Bodhisattva sculptures in the Main Hall. The study target is to reveal the craftsmanship and materials of the painted Bodhisattva sculptures. X-ray detection and the ground-penetrating radar were employed to explore the internal structure of the painted sculptures reasonably. Through microscope analysis, X-ray fluorescence spectrometer, X-ray diffractometer, scanning electron microscopy and infrared spectroscopic analysis, the chemical constituents and hierarchical structure of the pigment layer were detected and analyzed. The grain composition and chemical composition of the base layer were presented as well. The research results offer detailed documents for subsequent restoration and pave the way for preventive conservation. Finally, this paper summarized the craftsmanship and materials of painted sculpture works in different periods, so as to explore the development history of the painted sculptures culture.

Keywords: Fengguo temple, Painted sculptures, Liao Dynasty, Craftsmanship, Materials

Introduction

The Fengguo Temple is a Buddhist temple located in Yi County, Liaoning Province, northeast China. The temple was first built in the ninth year of Kaitai period of the Liao Dynasty (AD 1020) as a royal temple. Then it grew quite larger during the subsequent centuries. Today, only two halls, two gates, and a decorative arch survive. The most important surviving building is the Main Hall, which is notable for its wooden structure and the sculptures in it. In 1961, it was declared by the State Council as among the first batch of state priority protected sites. In 2013, the Main Hall was placed on China's tentative list for UNESCO World Heritage Site consideration, along with the Wooden Pagoda of Ying County [1].

In the 1930s, Japanese scholar Sekino Tadashi visited the Fengguo Temple. He unveiled the prelude to modern academic research on the Fengguo Temple, especially the Main Shrine Hall. For the first time, he published the plan view of the Main Hall [2] (Fig. 1e). In the 1950s, the Beijing Cultural Relics Organizing Committee conducted a detailed investigation and mapping of the Fengguo Temple [3]. By the end of the 20th century, the American scholar Steinhardt N. S. systematically inspected almost all the Liao Dynasty wooden structures. She believed that the Fengguo Temple had not received deserved attention from the academic community [4]. In 2006, the School of Architecture of Tianjin University and the China Cultural Heritage Research Institute used a variety of technical means including 3D laser scanning to conduct detailed

*Correspondence: yansj@cug.edu.cn
[1] Faculty of Engineering, China University of Geosciences (Wuhan), Hongshan District, Lumo Road, No 388, Wuhan 430074, China
Full list of author information is available at the end of the article

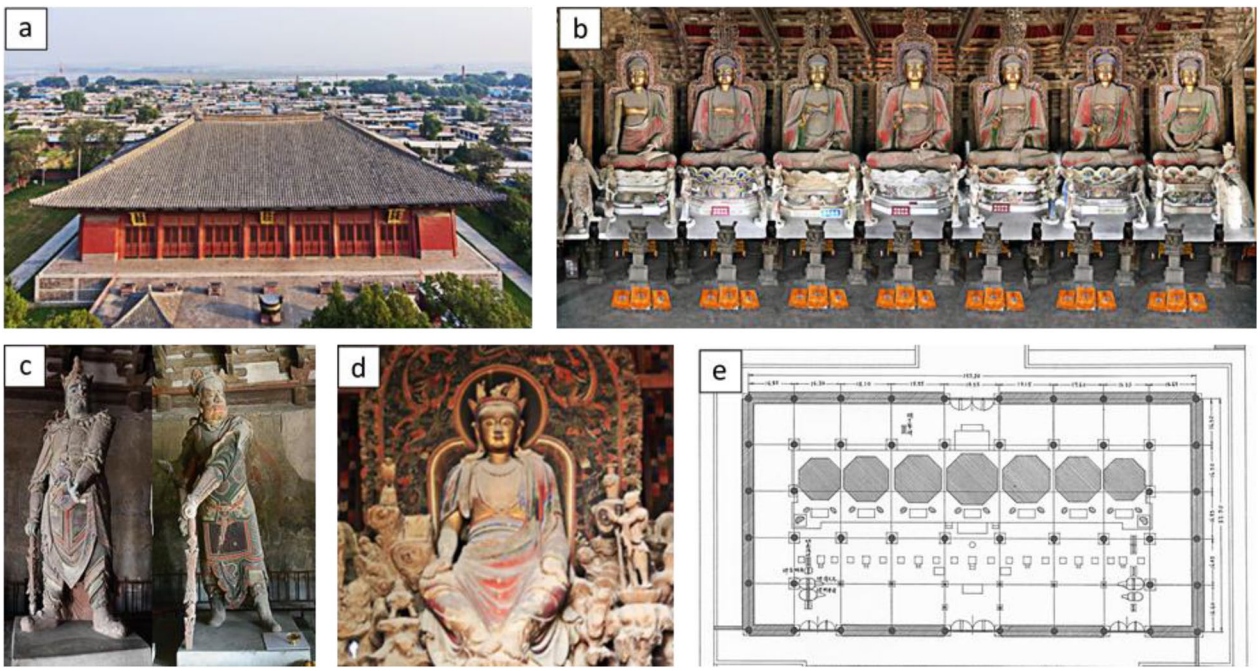

Fig. 1 Introduction of the Fengguo Temple (**a**) Landscape of the Main Shrine Hall (photoed by Shao Shihai from Talk Nanjing) (**b**) The painted sculptures of the Fengguo Temple (**c**) Two Guardian Kings (**d**) The Guanyin of the Ming Dynasty (**e**) The plan view of the Main hall firstly published by Sekino Tadashi [2]

surveys and obtained a large amount of physical data [5]. In recent years, some scholars analyzed the diseases and craftsmanship of the wall paintings in the Main Hall [6].

It is not difficult to find that the current research on the Fengguo Temple mainly lies in its wooden structure and murals, ignoring the precious painted sculptures in the Main Hall. According to the monuments and literatures, the Main Hall was repaired at least seventeen times between 1487 and 1888. In 1948, the Fengguo Temple was bombed because of the war. Fortunately and miraculously, the Main Hall was not destroyed. It was only repaired again in the 1980s [4]. The nature of the materials is critical for study the cultural relics. It would increase the understandings of the artisans' skills through ages, cultural influences and geographic regions. In addition, it is also the basis for selecting the most appropriate procedures and materials for restoration [7].

To date, many researchers have employed various technical means to study the production process and materials of the cultural relics [8]. They also studied the disease characteristics [9] and degradation mechanisms of the cultural relics [10]. Usually, each technical mean has its own areas of expertise. X-ray detection is often used to reveal the production process and internal defects of the cultural relics. It can extract the covered inscriptions and ornamentation on the surface of the cultural relics. Due to its penetrativity and nondestruction, X-ray detection could reflect the situation before and after the restoration. It could provide the internal information and the development of diseases of the cultural relics [11–15]. Some researchers employed ground-penetrating radar (GPR) to identify the position of the ancient tombs [16, 17] or buried bases of city walls, ditches, roads, etc. [18, 19]. Some heritage conservators once used GPR to measure the thickness of the base layer of the murals and confirm its feasibility [20].

As a common laboratory instrument, optical microscope (OM) is often used to study the mineral composition of ceramics and pigments [21, 22], casting technology and smelting level of metal cultural relics [23]. It has many applications in analyzing the change of the parameters of stone carving before and after weathering [24], and exploring the painting process of art works [25]. Generally, scanning electron microscope and energy dispersive spectrometer (SEM-EDS) are used for the observation and analysis of the microscopic morphology of pigment particles [26]. This method can also be applied to analyze the hierarchical structure of the pigment layer [27]. When the cultural relics are consolidated by some reinforcement materials, SEM-EDS could evaluate the effect before and after the reinforcement [28]. When investigating the cultural relics, SEM-EDS can help to identify the disease characteristics and disease products [29, 30].

In the field of conservation, X-ray fluorescence (XRF) can be used for the identification of the material and authenticity of the cultural relics [31]. It is helpful for the dating of the cultural relics [32], the origin of pigments [33], the production process of colored painting [34], the colouration mechanism of decoration porcelain [35], and comparing the similarities and differences of the creative techniques between different artists [36]. It provides scientific basis and technical guidance for the cultural relic protection and restoration technology. X-ray diffraction (XRD) can be conducted to analyze the materials of wall paintings [37], characterization of corrosion products grown on silver roman coins [38]. It can identify the crystallized salts on the weathered limestone and sandstone buildings [39]. As for infrared radiation (IR), it can be used to distinguish the binding media of ancient polychrome cultural relics [40] and identify and characterize sandstones used for buildings and monuments [41]. All of the above methods are used in this article. Sometimes these methods can be used separately, but most of the time they are combined. So the results are more comprehensive and persuasive.

This paper makes comprehensive use of the detection and test methods to study the craftsmanship and materials of the painted Bodhisattva sculptures in the Fengguo Temple. X-ray detection and ground-penetrating radar are mainly used to analyze the internal structure of the sculptures, so as to have a preliminary understanding of the production process. By means of optical microscope, scanning electron microscope, energy dispersive spectrometer, X-ray fluorescence, X-ray diffraction, and infrared radiation, the pigment layer and the base layer were analyzed in detail. It is helpful to identify the materials for making and repairing. This study can lay a solid foundation for the follow-up research on deterioration mechanism and restoration.

Materials and methods

The Main Hall and the painted sculptures

By 2020, the Main Hall (Fig. 1a) of the Fengguo Temple will be a thousand years old. As a masterpiece of ancient Chinese wooden structures, the Main Hall is a lively evidence of history and culture in the Liao Dynasty. It is a splendid Buddhist architecture created by Khitan, an ethnic minority living in border regions who inherited and developed the traditional culture of central China. The Main Hall demonstrates brilliant Chinese civilization in wooden architectures, sculptures and paintings. It highlights the superb technical and artistic level achieved in 11th century in China [1].

The Main Hall contains seven large sculptures of Buddhas (Fig. 1b). The Seven Buddhas used to be the long-term popular Buddhist art theme in the Wei and Jin Dynasty. Most of the existing cultural relics themed on the Seven Buddhas are murals and sculptures in the stone pagoda or grottoes. It is rare that constructing painted sculptures in the wooden building with such a grand scale. In addition to Sakyamuni, the six other Buddhas represented are Vipashyin, Sikhin, Visvabhu, Krakucchanda, Kanakamuni and Kashyapa [42]. Each of the Seven Buddhas is flanked by two Bodhisattvas. There are two Guardian Kings standing in the east and west of the Main Hall respectively (Fig. 1c). Behind the Seven Buddhas, a statue of Guanyin(who assumes the role of a savior in Chinese Buddhism) of the Ming Dynasty is facing the back door [4] (Fig. 1d). The average height of the Seven Buddhas is about 9.4 m, and the average height of 14 Bodhissatvas statues is about 2.5 m [42]. The painted sculptures of the Seven Buddhas are among the oldest, biggest and most beautiful group of sculptures in the world, which make the Main Hall different from other Buddhist temples. All the remains in the Main Hall preserve the cultural features of traditional Buddhist architecture of the Liao Dynasty. They also demonstrate the precious artistic and scientific information of the Liao Dynasty.

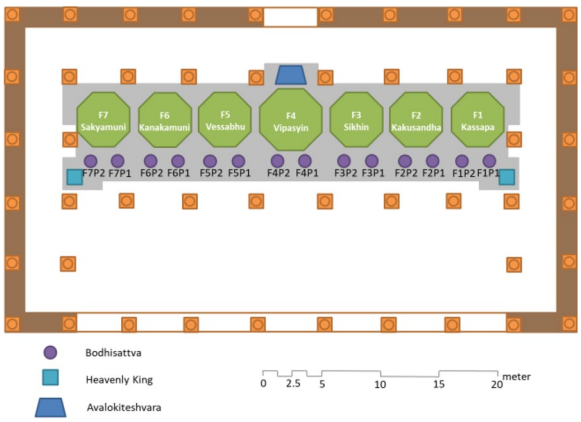

Fig. 2 The plan view of the Seven Buddhas and Bodhisattvas

Experimental methods

In order to determine the internal structure and connection type of the Bodhisattva, X-ray detection was conducted. Simultaneously, the ground-penetrating radar was used as a non-destructive method to assist the investigation of the internal skeleton structure and current situation of 14 Bodhisattvas. The Seven Buddhas are named F1, F2, F3, F4, F5, F6, and F7 from right to left in the picture. The 14 Bodhisattvas, arranged from east to west, are named F1P1, F1P2, F2P1, F2P2, F3P1, F3P2, F4P1, F4P2, F5P1, F5P2, F6P1, F6P2, F7P1, and F7P2, respectively.

F1P1 represents the left-hand side Bodhisattva of F1. The specific plan view of the statues is showed in Fig. 2.

X-ray detection

When the X-ray passes through the object being irradiated, its energy will be lost to some extent. If the textures, thickness, and density of the objects are different, the transmittance will vary and so will the grayscale of the pictures. Based on the grayscale images, the internal structure, the morphology, the material, and even the relative position relationship of the object could be interpreted and revealed, as well as the inner defects of the artworks and other valuable information [43].

The X-ray detector used in this investigation is from Dalian Xi'ao Testing Equipment Co., Ltd. The imaging system is from German DUERR Company. The model of the imaging plate is HD-IP Plus 35×42 cm, and the pixel size of the detection graph is 100 μm. When shooting, we put two imaging plates behind the sculpture in parallel and shoot from top to bottom. If the width of the sculpture is beyond the width of two imaging plates, we will reshoot for the excess part. Since the thickness in various parts of the painted sculpture is different, the exposure parameters during shooting are also different. Therefore the assembled X-ray pictures could only show the information of the internal structure. The contrast between different parts does not represent the difference in thickness. Here we took F4P1 as an example to make a detailed analysis of the internal structure and connection type of the painted sculptures. Because not every film can display valid information, we also chose the most clearly seen and characteristic images from F2P1, F3P2, F4P1, F4P2, F6P1, and F7P2 as assisted illustration.

Ground-penetrating radar

The ground-penetrating radar is a non-destructive detection technique. It uses high-frequency electromagnetic waves to detect the distribution and scale of hidden media, based on the electromagnetic differences between the detected object and its surrounding materials [44]. When the transmitting antenna emits high-frequency broadband short-pulse electromagnetic waves into the masonry, some electromagnetic waves are reflected at the interface with different dielectric properties. The receiving antenna receives the reflected echoes and records the reflection time [45].

We employed the equipment from RAMA/GPR radar of Sweden MALA Company and geological radar produced by IDS of Italy. Through the in-situ operation, we found that the ground-penetrating radar can only draw preliminary conclusions on the basic composition of the skeleton structures. It cannot be achieved to know whether the main skeleton is connected stably or the deterioration degree of the wood. The measurement work involves the horizontal and vertical measurements of the whole body. The work was conducted on the back of the Bodhisattva. We designed eight transverse measuring sections about 52 cm long and one vertical section about 180 cm long. The sketch map of the measuring lines is shown in Fig. 3. The frequency of the antenna is 1.6G; the maximum transmission rate is 400 kHz; time window 12 ns; sampling distance 2 mm; acceptance phase 270°; transmission phase 0°; and the distance is collected by the measuring wheel. Comprehensively considering the test results of 14 painted sculptures, this paper takes F2P2 and F5P2 as representative examples to infer the skeleton form of the painted sculptures.

Optical microscopy

Aimed to study the mineral composition and the granular component of the pigment layer and the base layer, we used different experimental methods, namely optical microscopy, scanning electron microscopy, X-ray fluorescence, X-ray diffraction, infrared spectroscopy and particle composition analysis. Applying these methods synthetically is helpful to know the materials of the painted sculptures more accurately. All the samples are collected from the damaged parts of the Bodhisattvas statues. Because the preservation status of painted sculptures is good, the number of samples is limited. Through

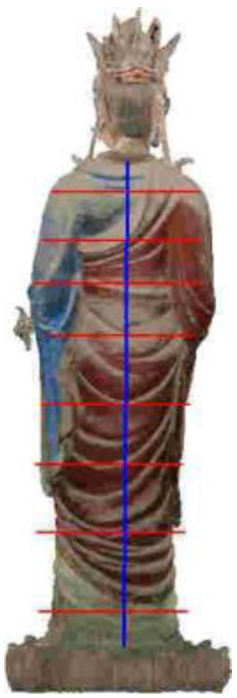

Fig. 3 The sketch map of the GPR measuring lines

Table 1 The sample list of optical microscopy

Sample number	Sample position	Colour
FGS-OM1	Left side of the left arm of F2P1	Green
FGS-OM2	Right side of the right elbow of F2P2	Blue
FGS-OM3	Ornament of F6P1	Blue
FGS-OM4	Right side of the dress in the crotch of F4P2	Green

Table 2 The sample list of scanning electron microscopy

Sample number	Sample position	Colour
FGS-SEM1	Left side of the left arm of F2P1	Green
FGS-SEM2	Right side of the right elbow of F2P2	Blue
FGS-SEM3	Back side of the dress in the right calf of F3P1	Blue
FGS-SEM4	Right side of the dress in the crotch of F4P2	Green

Table 3 The sample list of X-ray fluorescence

Sample number	Sample position	Colour
FGS-XRF1	Left back of F1P1	Red
FGS-XRF2	Bottom of the skirt of F3P2	Green

on-site investigation, it was found that the main colours of the pigment layer are blue, green and red.

The AXISKOP HBO 50 optical microscope made by Germany ZEISS Company was used in this study. Locations of the samples are listed in Table 1.

Scanning electron microscopy

In this experiment, we employed the ZEISS EVO MA25 scanning electron microscope, equipped with the Oxford X-Max 20 spectrometer. Experimental conditions: working voltage 20 kV, working distance 8.5 mm, and scanning time 100 s. The samples are listed in Table 2.

X-ray fluorescence

The elemental analysis of the painted sculptures was performed by X-ray fluorescence non-destructive testing. The portable X-ray fluorescence apparatus named Tracer III-SD is made by Bruker Company with an operating voltage of 40 kV, a current of 3 μA, and an analysis time of 30 s. The samples are listed in Table 3.

X-ray diffraction

The instrument we use is Rikagu SmartLab9 diffractometer made in Japan. The test scanning speed is 15°/min, step size 0.02, and scanning range 4°–70°. The samples are listed in Table 4.

Table 4 The sample list of X-ray diffraction

Sample number	Sample position	Colour
FGS-XRD1	Front side of the right thigh of F1P1	Green
FGS-XRD2	Left back of F1P1	Red
FGS-XRD3	Gathers of the dress of F2P1	Red
FGS-XRD4	Right back of F3P2	Blue

Table 5 The sample list of infrared spectroscopy

Sample number	Sample position	Colour
FGS-IR1	Front side of the right thigh of F1P1	Green
FGS-IR2	Outside of the right arm of F2P2	Blue

Infrared spectroscopy

The samples were analyzed via the Thermo Scientific Nicolet iN10 Infrared Microscope (Thermo Fisher, USA) under attenuated total reflection (ATR) mode, including MCT/A detector and BaF_2 window. Spectral acquisition parameters are: scanning times 32, gain 1, resolution 4 cm^{-1}, test range 4000–650 cm^{-1}. The pigment samples are analyzed and compared with the infrared standard atlas of minerals [46]. The samples are listed in Table 5.

Particle composition analysis

Grain composition of the base layer

To study the distribution ratio of the base layer, we took samples from the coarse clay layer and the fine clay layer. We referred to the method used in analyzing the base layer of murals [47]. Firstly, the sample is weighed, chopped and soaked in the purified water. Secondly, the experimenter stirs the mixture vigorously and separated the floating fibers quickly after the deposition for a while. Thirdly, the water with suspended silt is removed. The fibers are dried, weighed and identified. Repeat the above procedures until the water is substantially clear. The water in the sand and silt is separately removed by sedimentation. The quality of the silt and sand in the base layer can be weighed after drying.

Mineral chemical composition of the base layer

The instrument is D/MAX-2500 X-ray diffractometer made by Rikagu Corporation of Japan. During sample preparation, the sample was placed in a mortar and ground into powder severally, then placed on a glass slide, and placed into the instrument for testing. The voltage is 40 kV; the current is 200 mA, graphite monochromator filter, Cu target. JCPDS method was used for

phase analysis, and basic strength comparison method was used for quantitative analysis.

Results

Structure of the painted sculptures

X-ray detection analysis

To explore the manufactured process of these painted sculptures, X-ray detection was conducted. Bodhisattva F4P1, taken as an example here, provides some useful information (Fig. 4a). The analysis results showed that the base layer was directly attached to the wood skeleton (Fig. 4b). We found the wood skeleton in the head, chest, abdomen, arms, and legs. So the main body of the sculpture is wooden skeleton. There is only one wooden skeleton running through the chest (Fig. 4c & d). While there are stitching traces of wood skeleton in the part of arms, abdomen, and legs. The wood skeletons of the upper and lower arms are connected by metal connectors (Fig. 4e). There is an intact iron wire in the left arm of Bodhisattva F4P1, extending from the shoulder to the hand. The wooden skeleton does not extend to the hand. Furthermore, there are no cracks on the base layer at the end of the hand (Fig. 4f). In addition, the left chest of F4P1 is dark and the base layer is relatively thin. There is an ancient coin in the middle of the chest (Fig. 4f). It can be clearly seen that there are different levels of cracks in the right shoulder, left arm, wrists and other positions (Fig. 4f).

When performing X-ray detection on other statues, the regular patterns of the internal structure could be found. It could be seen that the main body inside the sculpture is wooden skeleton. The base layer is directly attached to the wooden skeleton, and there are cracks of different degrees in the base layer (Fig. 5a & e). There is a central column running through the painted sculpture, and the wooden skeletons are mainly connected by metal connectors (Fig. 5a & d). All the internal skeleton of the instruments are iron wires, which is convenient for modeling (Fig. 5c). The ancient coin mixed in base layer of the F7P2 indicates that the trace of maintenance (Fig. 5b).

Ground-penetrating radar analysis

The horizontal profiles of F2P2 are shown in Fig. 6. The obvious columnar reflection anomalies are indicated by red squares. There are three reflection anomalies in the first five profiles, one anomaly in the sixth profile, and two anomalies in the seventh and eighth profiles. Hence, we inferred that there are three columns in the upper body, one column runs through the hips to the knees, and two columns in the lower part.

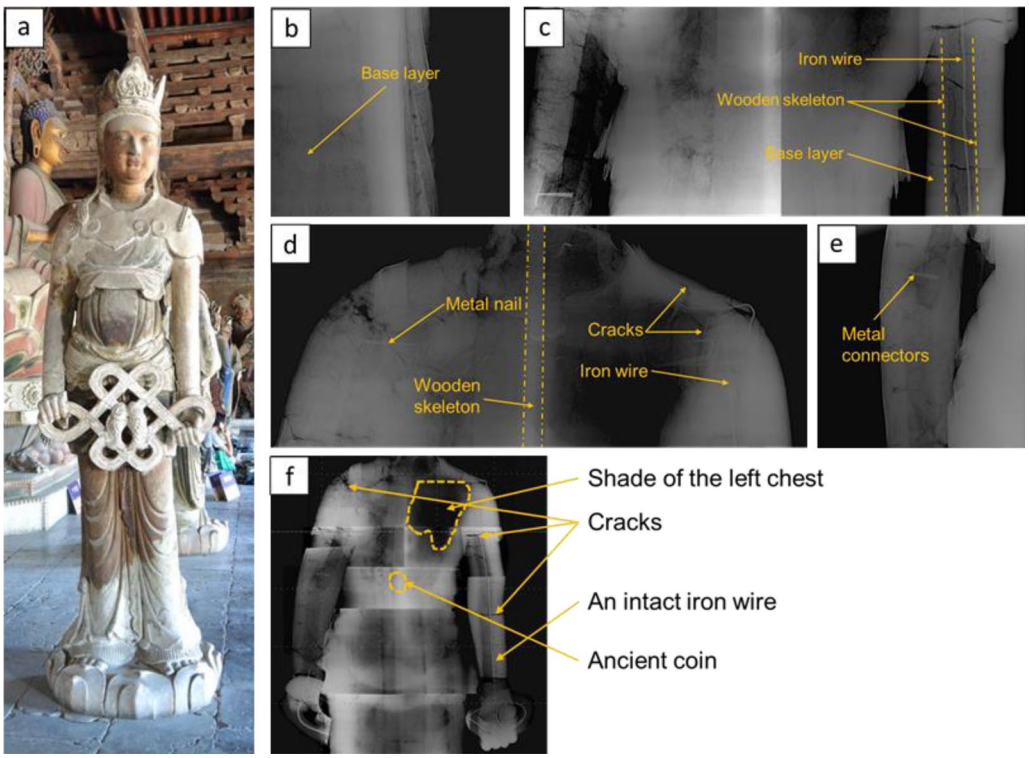

Fig. 4 X-ray detection of F4P1 (**a**) Bodhisattva F4P1 (**b**) X-ray film of F4P1's right thigh (**c**) X-ray film of F4P1's chest and upper arms (**d**) X-ray film of F4P1's shoulders (**e**) X-ray film of F4P1's right arm (**f**) X-ray film of F4P1's upper body

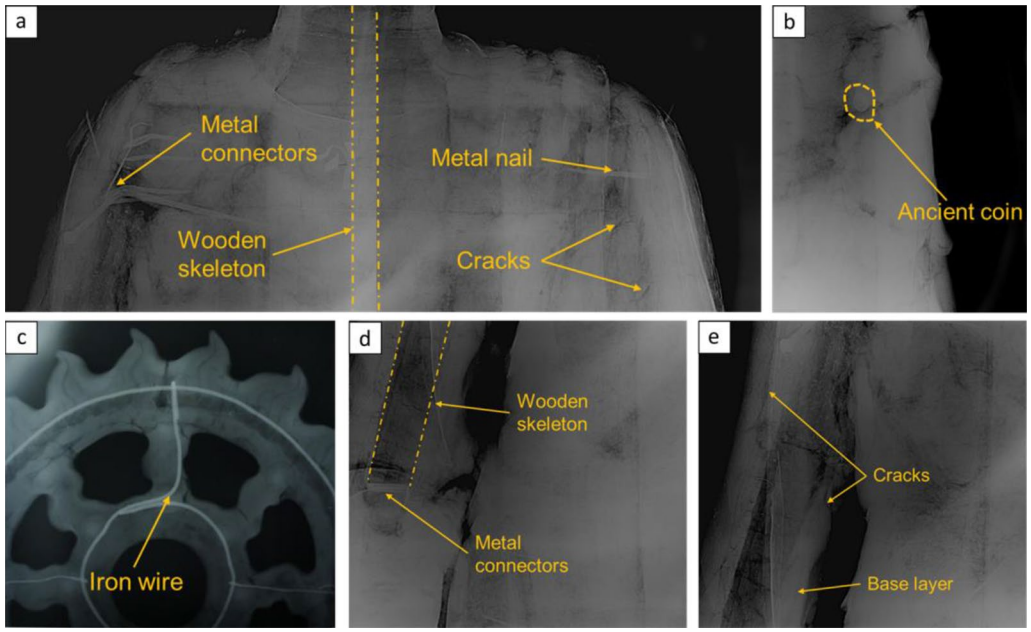

Fig. 5 X-ray detection of other Bodhisattva (**a**) X-ray film of F6P1's chest and upper arms (**b**) X-ray film of F7P2's left shank (**c**) X-ray film of F4P2's instrument (**d**) X-ray film of F6P1's left arm (**e**) X-ray film of F6P1's left arm

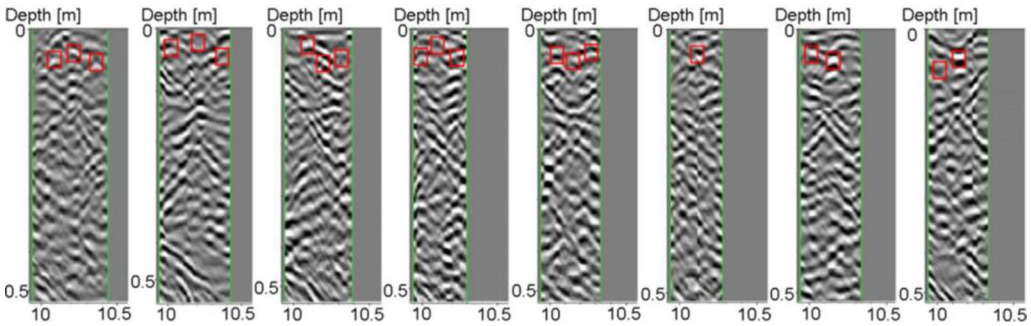

Fig. 6 The horizontal profiles of F2P2

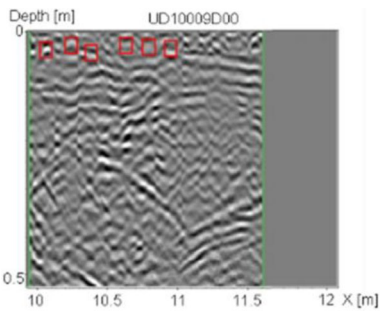

Fig. 7 The vertical profile of F2P2

The vertical measurement of F2P2 is shown in Fig. 7. There are six obvious lateral anomalies in the profile. On the right side of the profile, that is the leg of the sculpture, there are many lateral anomalies with a width of about 10 cm. Between these anomalies, there are gaps less than 1 cm. We inferred that there are two vertical columns in the part of legs. The horizontal wood boards might connect between two columns.

The horizontal profiles of F5P2 are shown in Fig. 8. There are three reflection anomalies in the first four profiles, two anomalies in the fifth profile, and one anomaly

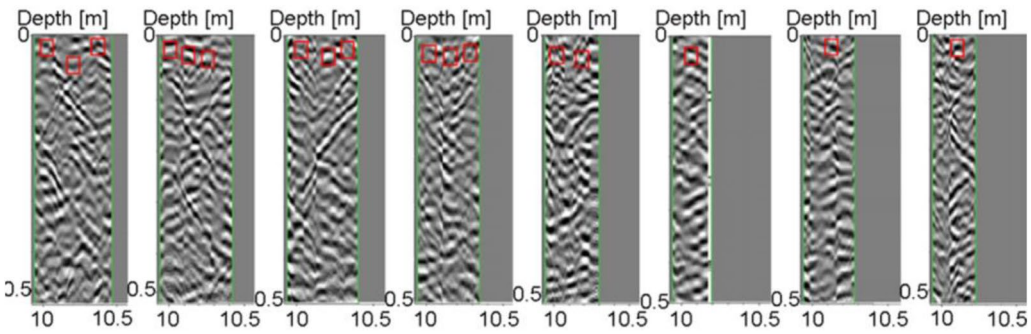

Fig. 8 The horizontal profiles of F5P2

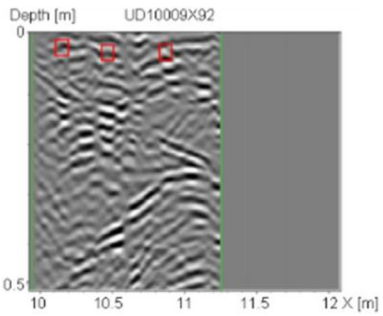

Fig. 9 The vertical profile of F5P2

in the last three profiles. Hence, we inferred that there exist three columns in the upper body, two columns run through the hips to the knees, and one column in the lower part.

The vertical measurement of F5P2 is shown in Fig. 9. There are three obvious lateral anomalies in the profile. On the right side of the profile, that is the leg of the sculpture, the reflecting layer is obvious and even. The horizontal connection is weak. This anomaly is possibly caused by a vertical wood board. We inferred that there are vertical boards in the part of leg.

By using Photoshop, a composite of the radar images of the upper and lower body are achieved. In the process of synthesis, the corner of the Bodhisattva's left shoulder is taken as the base point to correct and stitched the images together. All the information is based on the abnormal amplitude and abnormal width. Adding random disturbances, we perform correlation analysis and gridding. Finally, we draw images of the skeleton structure of the sculptures. The inferred skeleton structures of F2P2 and F5P2 are shown in Fig. 10. It is clear that the upper part of the Bodhisattva is a frame structure connected by wooden boards. But the structure of the lower body is different. The center pillar of F5P2 runs through the whole body, while that in F2P2 doesn't.

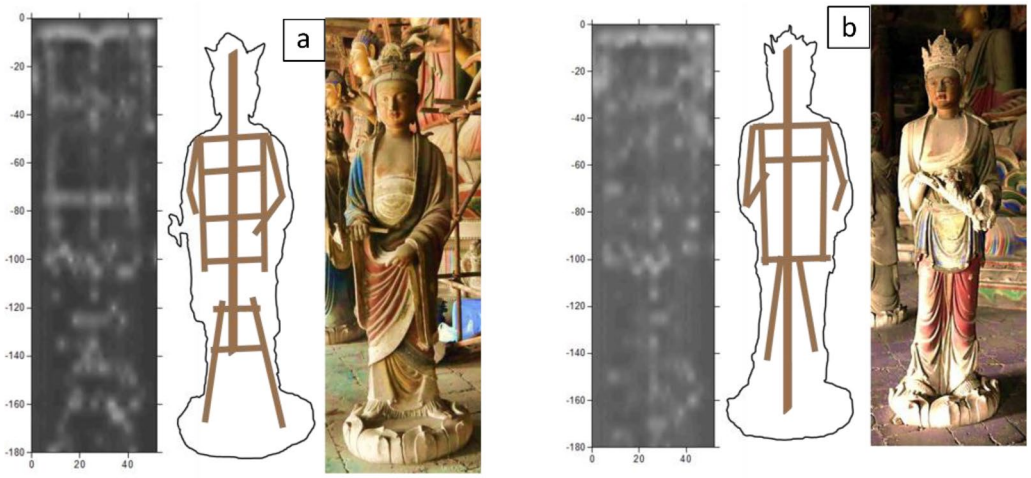

Fig. 10 The inferred skeleton structure of Bodhisattvas (**a**) Bodhisattva F2P2 (**b**) Bodhisattva F5P2

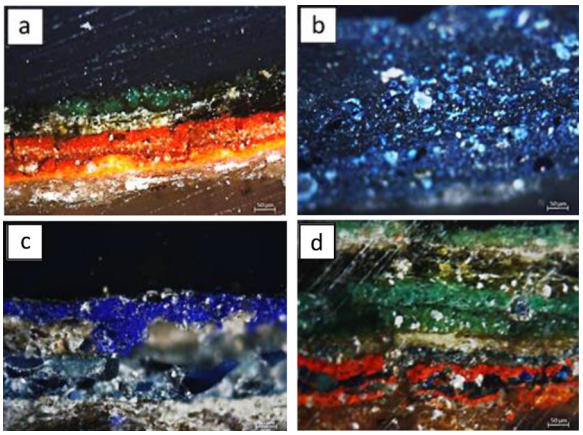

Fig. 11 Optical microscopy pictures of pigment (**a**) FGS-OM1 (Green) (**b**) FGS-OM2 (Blue) (**c**) FGS-OM3 (Blue) (**d**) FGS-OM4 (Green)

Material analysis of the painted sculptures

Profile analysis of pigment

We took 4 pigment samples from the damaged parts of F2P1, F2P2, F6P1, and F4P2. The optical microphotographs showing the stratigraphy of each sample are shown in Fig. 11.

The colour of the sample refers to colour that the top layer displays. From the optical microphotographs, some samples show the stratigraphy of the pigment layer, indicating that in different historical periods, the craftsmen have ever repaired the painted sculptures and used different pigments. In Fig. 11a, the particles of the green sample are fine. There is a red strip under the green pigment. The orange-red pigment is primed, and the red pigment is laid on it. The thickness of this layer is relatively uniform. Below the red pigment is the mottled plaster and fine clay layer. In Fig. 11b, the particles of this sample are fine and the whole colour is bright. In Fig. 11c, the upper layer is dark blue, and the lower layer is light blue. There are indistinct traces of the plaster between these two layers. In Fig. 11d, scratches appear on the surface of the sample. Between the green pigment and the combination of orange-red pigment and red pigment, there is a thin base layer. There are also blue pigment mixes in it. The microscope can only show the colour and stratigraphy of pigments. It is still difficult to judge exactly what the mineral is.

SEM-EDS analysis

To analyze the pigment layer from the microscopic view, we used the scanning electron microscope. It can distinguish the morphology and distribution of the pigment crystal. We took 4 pigment samples from the damaged parts of F2P1, F2P2, F3P1, and F4P2. Among them, samples FGS-SEM1, FGS-SEM2, FGS-SEM3 correspond to samples FGS-OM1, FGS-OM2, FGS-OM3 in the profile analysis, respectively. The results are shown in Table 6.

Figure 12a shows that the delamination phenomenon of the pigment is obvious. The pigment layer is in mixed contact with the plaster and the base layer. This should attribute to "compressing" during the production process [48]. The EDS results show that the content of carbon and oxygen are high. Among them, Mg, Al, Si, K, and Ca should come from humus. The characteristic elements are chlorine and copper. It is speculated that the mineral component may be atacamite ($Cu_2(OH)_3Cl$).

Figure 12b shows that the mineral particles of FGS-SEM2 are uniform and fine. There is only one mineral pigment in the viewing zone. The EDS results show that the contents of carbon and oxygen are high. The characteristic element is iron. According to the references, the common blue pigments in ancient China are Chinese blue, lazurite, azurite, smalt, ultramarine and Prussian blue [49]. Among them, only the Prussian blue contains Fe element. Therefore, it is preliminarily assumed that the mineral composition of the blue pigment may be Prussian Blue ($Fe_7(CN)_{18}{\bullet}14H_2O$).

FGS-SEM3 is also a blue pigment. The delamination phenomenon in Fig. 12c is relatively clear. The crystal particle size is heterogeneous. The particles taper off from top to bottom, which should be the traces of repair in different ages. The EDS results show high carbon and oxygen content. It contains the characteristic elements of chlorine and copper. Since this sample is blue and it contains a high amount of copper, it is reasonable to speculate that it is a mixture of atacamite ($Cu_2(OH)_3Cl$) and azurite ($2CuCO_3{\bullet}Cu(OH)_2$).

Figure 12d shows that the thickness of each pigment layer is relatively average. It is the evidence of painting

Table 6 The SEM-EDS analysis results of the pigments layer of Bodhisattvas (wt%)

Sample number	Sample colour	C	O	F	Fe	Mg	Al	Si	S	Cl	K	Ca	Cu
FGS-SEM1	Green	33.30	48.69	1.29	–	4.36	0.72	4.86	0.77	0.24	0.44	2.90	2.43
FGS-SEM2	Blue	53.94	35.63	–	1.58	3.09	0.43	3.34	0.41	0.14	–	1.44	–
FGS-SEM3	Blue	32.21	47.91	–	–	1.63	0.27	1.98	0.80	5.58	–	0.98	8.64
FGS-SEM4	Green	51.61	35.78	–	0.59	1.05	1.24	3.51	1.08	1.37	0.25	0.97	2.55

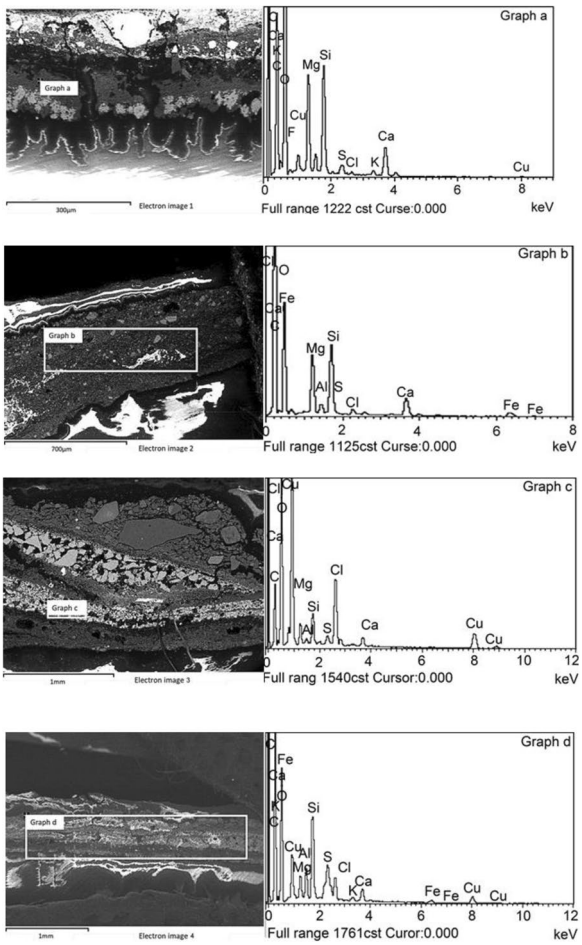

Fig. 12 SEM-EDS images of 4 pigment samples (**a**) EDS spectrum of FGS-SEM1 (Green) (**b**) EDS spectrum of FGS-SEM2 (Blue) (**c**) EDS spectrum of FGS-SEM3 (Blue) (**d**) EDS spectrum of FGS-SEM4 (Green)

more than once. The EDS results show high content of carbon and oxygen, accompanied by the characteristic elements of chlorine, copper. The ratio of chlorine to copper is close to 1:2. Considering that this pigment sample contains other oxygen compounds, it will increase the content of oxygen. Therefore, it is presumed that this pigment sample contains atacamite ($Cu_2(OH)_3Cl$).

X-ray fluorescence (XRF) analysis

Figure 13 and 14 show XRF results for the red pigment in F1P1 and the green pigment in F3P2. Figure 14 shows that the coloring elements are Fe, Hg, and Pb. According to the types of mineral pigments commonly used in ancient China, it is speculated that the mineral pigments may be cinnabar, minium, and iron oxide red. As can be seen from Fig. 14, the coloring elements are Cu, Fe, Pb, and Ca. It is supposed that the mineral pigments may be malachite, atacamite, minimum, and gypsum. In order

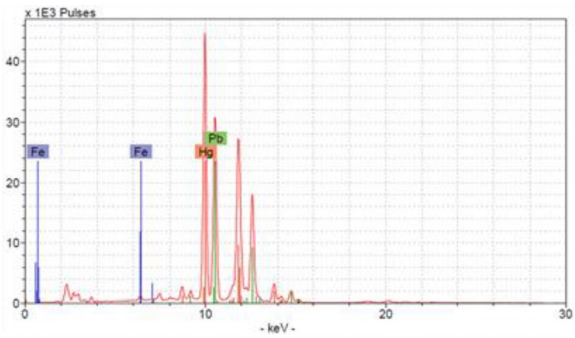

Fig. 13 The XRF spectrum of FGS-XRF1 (Red)

to further determine the specific mineral composition of the pigments, we need to carry out other experiments.

X-ray diffraction (XRD) analysis

The experimental results of XRD are shown in Table 7and Fig. 15. It should be noted that sample FGS-XRD2 corresponds to sample FGS-XRF1 in the XRF analysis. The results indicate that the mineral composition of the green pigment is atacamite. It is consistent with the results of scanning electron microscopy. The mineral composition of the red pigment includes cinnabar and minium. It is in line with the results of X-ray fluorescence. The main mineral composition of the blue pigment is Prussian blue. It is in accordance with the observation of scanning electron microscopy.

Infrared analysis

Infrared spectroscopy can determine the chemical composition of a substance. The parameters are obtained by absorption of infrared light by molecules. The results are based on the position, intensity, and shape of the band frequency [50, 51].

According to relevant literature [52], the infrared spectral characteristic peaks of the atacamite in the

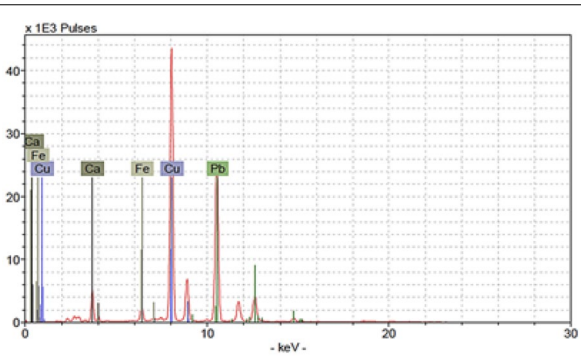

Fig. 14 The XRF spectrum of FGS-XRF2 (Green)

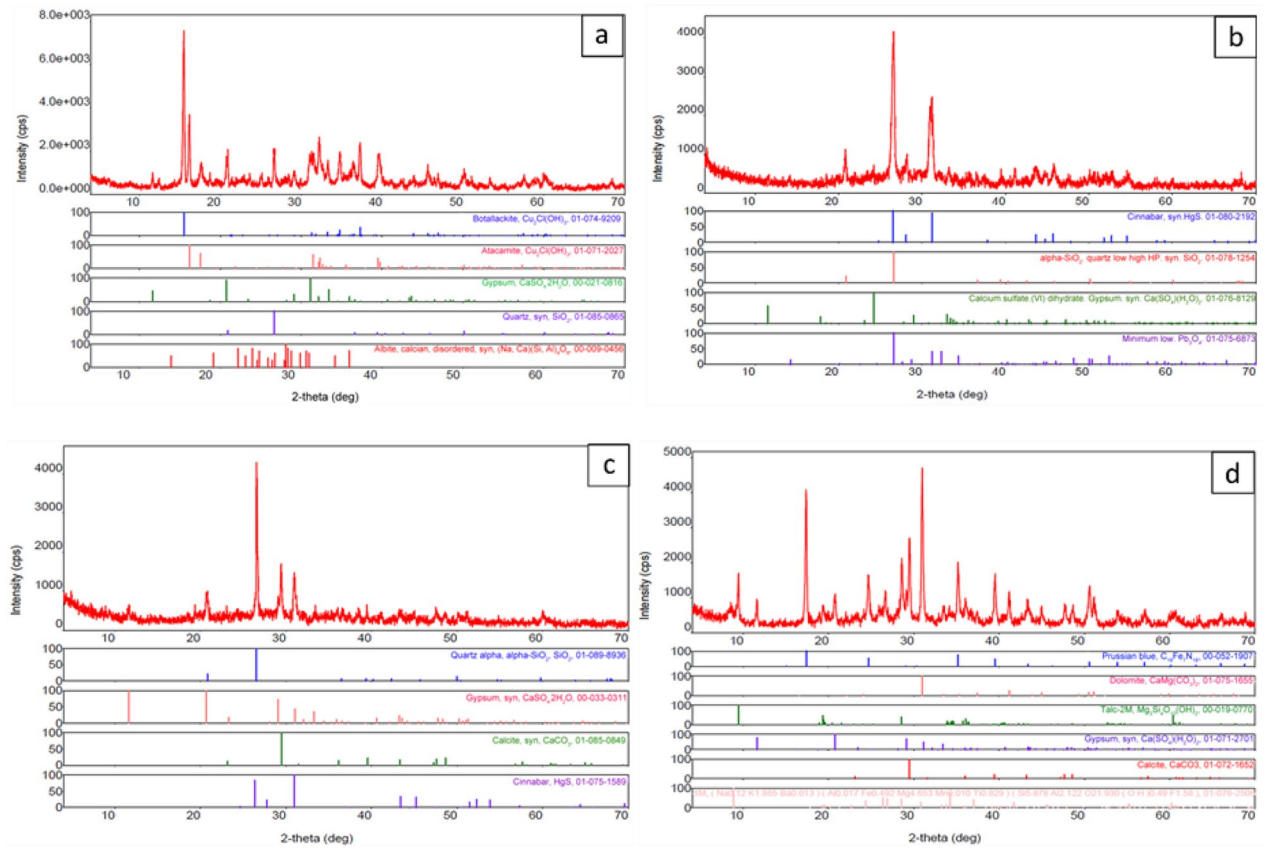

Fig. 15 XRD patterns of different pigments (**a**) FGS-XRD1 (Green) (**b**) FGS-XRD2 (Red) (**c**) FGS-XRD3 (Red) (**d**) FGS-XRD4 (Blue)

Table 7 XRD analysis results of the pigments layer of Bodhisattvas

Sample number	Sample colour	Test results
FGS-XRD1	Green	Atacamite, Quartz, Gypsum, Feldspar
FGS-XRD2	Red	Cinnabar, Quartz, Gypsum, Minium
FGS-XRD3	Red	Cinnabar, Gypsum, Calcite, Quartz
FGS-XRD4	Blue	Prussian blue, Calcite, Gypsum, Dolomite, Talc, Mica

fingerprint region include 985, 948, 914, 894, 849, and 819 cm^{-1}, as shown in Fig. 16a. It should be noted that sample FGS-IR1 and sample FGS-XRD1 are from the same location. Combining with the previous test results of XRF, SEM, and XRD on the green pigment, it is confirmed that the green mineral pigment is atacamite. Figure 16b shows that the characteristic absorption peak of the cyano group in the metal complex is near 2087 cm^{-1}, indicating that there may be Prussian blue in the sample.

Particle composition analysis

From the broken part of the sculptures, we can see clearly that the base layer is divided into two parts: the coarse clay layer and the fine clay layer. The thicknesses of both layers vary at different positions, with the former ranging from 3 to 10 cm and the latter from 0.5 to 1.0 cm.

We analyzed the grain composition of the base layer. The results are shown in Table 8. The coarse clay layer is mixed with wheat straw, with a reinforcement rate of about 3 %. The fine clay layer is added with hemp with a reinforcement rate of about 2%. In general, the reinforcement of the base layer can effectively increase the tensile strength of the soil and improves the shrinkage resistance of the soil. Sand is also added to the fine clay layer to increase its resistances to shrinkage, strength and weathering.

The mineral chemical composition of the soil determines its basic properties [53]. In order to know the mineral composition of the base layer, we performed X-ray diffraction experiments on the samples of the coarse clay layer and the fine clay layer. The results show that the coarse clay layer mainly includes quartz, feldspar, calcite, gypsum, and illite (Fig. 17a). The main mineral

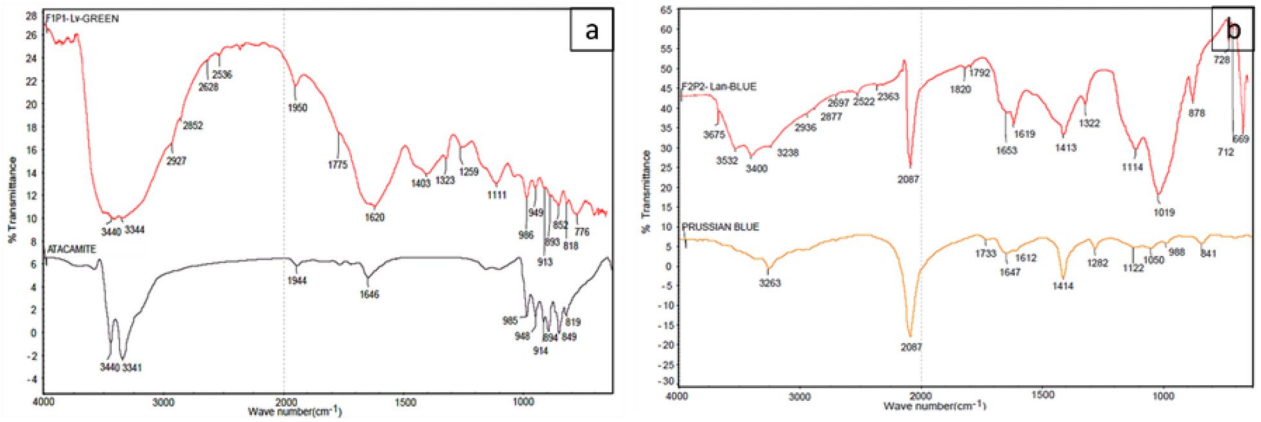

Fig. 16 The infrared analysis curves of pigments (**a**) FGS-IR1 (Green) (**b**) FGS-IR2 (Blue)

Table 8 The grain composition of the course layer and fine layer of Bodhisattva

Sample number	Total weight(g)	Soil weight(g)	Sand weight(g)	Fiber weight(g)	Type of fiber
FGS-CL1	15.76	15.22	/	0.54	Wheat straw
FGS-FL1	6.68	3.25	3.40	0.13	Hemp

components of the fine clay layer are quartz, feldspar, and illite (Fig. 17b).

Discussion

The craftsmanship and materials of the painted sculptures in the Fengguo Temple

Environmental factors are the external conditions for the occurrence of diseases, while the physical and chemical

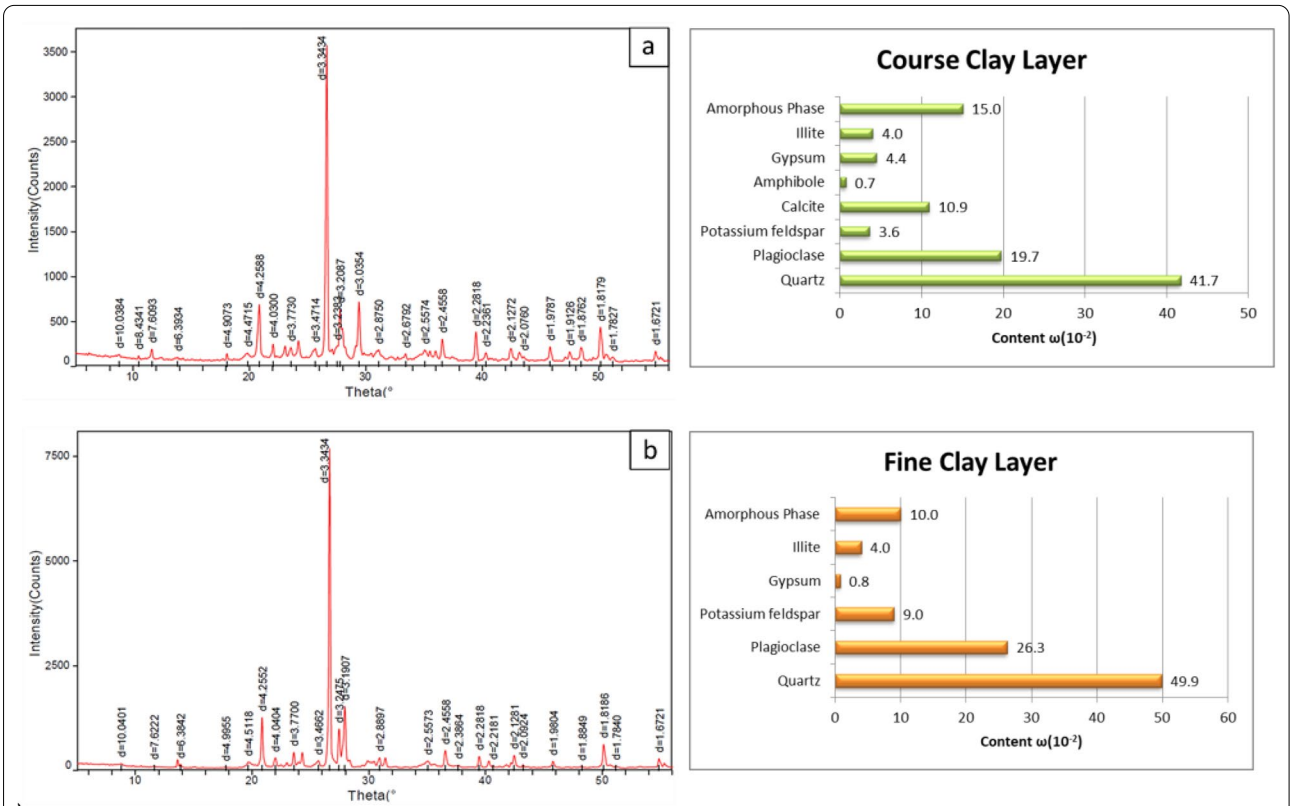

Fig. 17 The XRD patterns and analysis results of the base layer of Bodhisattvas (**a**) FGS-CL1 (**b**) FGS-FL1

characteristics of the materials of the painted sculptures are the internal fundamental factors of the diseases [54]. Through the discussion on the craftsmanship and materials of painted sculptures, the scientific connotation contained in the traditional techniques can be explained. It will provide some quantitative basis and technical guidance for the protection of painted sculptures in ancient temples.

Structure of the wooden skeleton

The scale, shape, weight capacity, stability, and durability of the painted sculpture are all closely related to the construction of the wooden skeleton [54]. Through X-ray detection and ground-penetrating radar analysis, the wood skeleton structure of the painted sculpture was basically determined. Firstly, the base layer is directly attached to the wood skeleton, and there are cracks of different degrees in it. Secondly, there is only one vertical wood skeleton. Other wood skeletons are connected by metal connectors. Thirdly, the structure of the upper body of the wood skeleton is similar but not regular and the lower body can be distinguished by the wood skeleton runs through or not. Finally, the ancient coins from the base layer can be used as a judgment basis for historical restoration. Compared with the craftsmanship of other dynasties, the painted sculptures in the Fengguo Temple lack the step of winding or binding straw rope around the wooden skeleton [55]. During the on-site investigation, we found the base layer detached from the wooden skeleton in some locations. This may be concerned with the missing step. There are many functions of winding or binding straw rope around the wooden skeleton. It can enhance the adhesion of base layer when molding and help the clay hang on the skeleton. It can fill the inner space of the painted sculpture to reduce the weight and thickness. When the wet base layer gets thoroughly dried and shrinks, the straw rope can prevent the base layer from detaching from the wooden skeleton to some extent. The straw rope is breathable and the water evaporates easily. Therefore, the wooden skeleton inside is not easy to decay [54]. From the films of the X-ray detection, we could find many traces of historic repair. For example the ancient coin in the base layer, it represents the respect and worship for the Bodhisattva by artisans when repairing. Different levels of cracks in different position cannot be ignored. The cracks will become the emphasis of subsequent repair. The X-ray detection can only inspect the local characteristics of painted sculptures. As for the overall shape of the wooden skeleton, conjoint analysis needs to be performed by ground-penetrating radar.

By analyzing the anomalies of the profiles, we inferred the wooden skeleton roughly. The number of the anomalies stands for the number of the columns in the upper and lower parts. Furthermore, we drew images of the inferred skeleton structure of the painted sculptures. Through the investigation and analysis of 14 Bodhisattvas, it is found that the upper part of the sculpture was similar but irregular. The upper structure of F1P1, F1P2, F3P1, F3P2, F4P1, F5P1, F6P1, F6P2, F7P1, and F7P2 is made up of 4 horizontal columns. The upper structure of F2P1, F2P2, and F5P2 consist of 3 horizontal columns, while the upper structure of F4P2 consist of 5 horizontal columns. The lower part can be basically divided into two types, with a penetrative pillar or not. The center pillar of F1P1, F1P2, F2P1, F3P1, F5P1 and F5P2 runs through the whole body, while other painted sculptures doesn't. It is obvious that when making the wooden skeleton, there was no uniform standard and model. The craftsmen built the internal structure according to the actual situation of each painted sculpture and their own experience.

Characteristics of the pigment layer

A series of analyses were conducted on 14 pigment layer samples. We aim to analyze the micro morphological characteristics and mineral composition of the pigment layer comprehensively. The samples are available in red, green and blue colours. Based on the comprehensive experimental results, we have basically determined that the corresponding mineral components of red, green and blue are cinnabar & minium, atacamite and Prussian blue. Each colour in turn is discussed below.

Due to the small number of red samples, we only performed XRF and XRD experiment. From the experimental results, it is clear that the main mineral composition of red pigment is cinnabar and minium. Through profile observation, we found that sometimes cinnabar and minium are mixed. Always, minium is the base and cinnabar is on it. We also found red pigment under the green samples. This proves that the painted sculptures were repainted in history. Cinnabar is popular in ancient China because of its bright color and stable chemical properties [56]. After the First Emperor of Qin unified the country, the production of cinnabar and mercury developed rapidly. Cinnabar was used as pigment in the Terracotta Army [57]. Since the Wei, Jin, and Northern and Southern Dynasties, cinnabar has been used as mineral pigment in wall paintings in grottoes, tombs, temples, and palaces throughout the country [58, 59]. Minium is the subsidiary product of alchemy. It is an artificial pigment. Although its colour is bright, its chemical property is unstable [60]. Discoloration and degradation are common in murals around the world [61–63]. Mogao Grottoes used minium extensively in the prosperous Tang Dynasty [64]. Su et al. found that if minium was used alone in the murals, orange would convert to black completely. If minium was mixed with cinnabar or

iron oxide red, it could keep its original color [65]. Giovannoni believed that when lead pigment was mixed with other pigments, the later pigments served as a barrier to lead pigment [66]. Therefore, through the profile observation we found that the minium under the cinnabar was without discoloration.

Aiming at the green samples, we performed a comprehensive experimental analysis. Combining with the previous test results of XRF, SEM, and XRD on the green pigment, it is confirmed that the green mineral pigment is atacamite. Atacamite was used earliest in the murals and painted sculptures of Binglingsi Grottoes. It was used most widely in grottoes and tombs of Hexi Corridor, and in the Mogao Grottoes for the longest time. Since the Tang Dynasty, atacamite has been the main green pigment in the grottoes of Xinjiang. It is consistent with the literature about the records of production and sales [67].

When analyzing the blue samples, the test results showed that it was a mineral pigment containing iron. We also found that the infrared spectrum of the blue sample coincided with Prussian blue basically. In addition, the chemical composition of Prussian blue is ferric ferrocyanide. So we inferred that the mineral composition of the blue pigment was Prussian blue. It was discovered by a German named Diesbach when he was preparing red pigment in the 18th century [68]. As the first synthetic pigment in the modern sense [69], Prussian blue can not only replace expensive traditional blue pigment but also be used to judge the age limit of Western artifacts and artworks [70]. According to relevant studies, in the 1750s to 1770s, Prussian blue was introduced to China by the Swedish East India Company [71]. In the reserve painting on glass of the Cuishang Tower and the Chinese pawn tickets in the Qing Dynasty, the researchers found the use of Prussian blue [72, 73]. It is concluded that the blue pigment of the painted sculptures may be repainted. It was repaired in the Qing Dynasty [3].

Characteristics of the base layer

According to the observation of the samples, the base layer of the painted sculpture is divided into two parts: the coarse clay layer and the fine clay layer. The coarse clay layer is mixed with wheat straw, which is helpful for preventing shrinkage and hanging on the skeleton. The fine clay layer is added with hemp, which is conducive to subsequent painting because it enhances the smoothness of the base layer.

As for the mineral composition of the base layer, the coarse clay layer mainly includes quartz, feldspar, calcite, gypsum, and illite. Among them, quartz and feldspar belong to the original mineral. They are in good property of anti-weathering. Calcite is the particles of insoluble salt. It may be produced by adding lime during the production of base layer and the lime transforms to calcium carbonate. It can enhance the material strength and provide convenience for construction. Illite is a kind of clay mineral. It is the main source of colloidal particles in the soil particles, improving the plasticity of the base layer. The sample of the coarse clay layer may mix a little plaster, so the results include gypsum. The main mineral components of the fine clay layer are quartz, feldspar, and illite. It is similar to the coarse clay layer. The fine clay layer is the connection between the pigment layer and the coarse clay layer. Its strength requirement is not as high as the coarse clay layer, but it is expected to be flat. The lime used to increase strength in the coarse clay layer does not appear in the fine clay layer.

In the base layer, we detected illite without montmorillonite and kaolinite. It is known that montmorillonite has the most dramatic shrink-swell capacity. Hence, the clay with high montmorillonite content is not suitable for sculptures, although it has high viscosity. If the content of kaolinite and illite is relatively high in clay, it has moderate viscosity and good plasticity. It is suitable for making sculptures. Therefore, it is one of the reasons why the painted sculptures in the Fengguo Temple could survive thousands of years.

Generally speaking, when constructing clay sculptures and murals, the raw material of the base layer is selected locally [74–76]. Therefore in the follow-up research, local soil samples can be selected and analyzed to determine the source of the base layer.

Manufacturing process

According to the field investigation, as well as the X-ray detection, it is summarized that the moulding sequence of the painted Bodhisattvas sculptures in the Fengguo Temple is wood skeleton→ coarse clay layer→ fine clay layer→ plaster→ pigment layer (from inside to outside) (Fig. 18).

Throughout the painted sculptures in the Fengguo Temple, we can know about the artistic style of painted sculptures in the Liao Dynasty. The painted sculpture has a dignified appearance, with a sense of volume. The ornaments are gorgeous and rich. The belt and the skirt for fighting and hunting are distinguish from other periods. The style of costume is similar to that of the generals during the Tang and Liao Dynasty. This multi-ethnic fusion style is a transformation of Indian Buddhist statues by Khitan nationality [77] (Fig. 19c).

The craftsmanship of painted sculptures in temple in other dynasties

The Tang Dynasty

The art of painted sculptures developed to a peak stage in the Tang Dynasty. The style of Buddhism statues in this

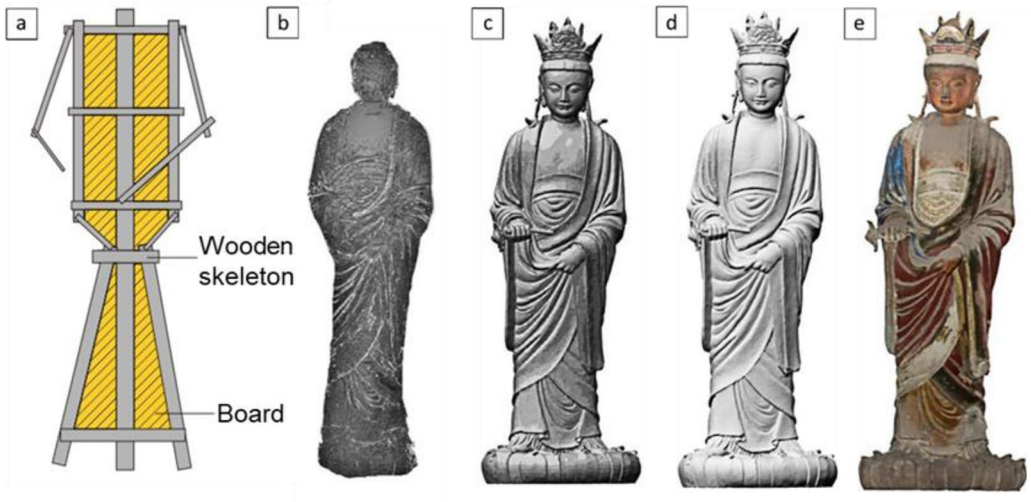

Fig. 18 The making process of the Bodhisattvas in the Fengguo Temple: (**a)** wooden skeleton (It only represents the first step of the production sequence is to build a wooden skeleton, and does not represent the specific structure of each painted sculptures) (**b)** coarse clay layer (**c**) fine clay layer (**d)** plaster (**e**) pigment layer

Fig. 19 The painted sculptures in temples of different dynasties: (**a)** Qinglian Temple (Tang Dynasty) (**b)** Chongqing Temple (Song Dynasty) (**c**) Huayan Temple (Liao Dynasty) (**d**) Jade Emperor Temple (Yuan Dynasty) (**e**) Shuilu'an Temple (Ming Dynasty) (**f**) Houtu Temple (Qing Dynasty)

period was majestic, strong, and extraordinary. The style that prevailed in the late Tang Dynasty was dignified and gentle [78]. Taking the sculptures in the Qinglian Temple as an example (Fig. 19a), the moulding sequence is wood skeleton→ straw mat→ coarse clay layer→ fine clay layer→ pigment layer (including plaster). The researchers found the processing method was different for the coarse clay layer and the fine clay layer. The coarse clay layer had higher quartz content than the fine clay layer. It indicated that sand was added to prevent excessive shrinkage when making the coarse clay layer. The fine mud layer had higher calcite content and lower quartz content. It showed that the fine mud layer was not only sieved, but added lime to form calcium carbonate. The artisans hanged straw mat on the wooden skeleton and fixed it with straw rope. The straw mat was woven with reed stem. It is more beneficial to hang clay on the skeleton [79]. This step is different from other dynasties.

The Song Dynasty

In the Song Dynasty, the style of painted sculpture had a big change. The figures are of fine appearances and handsome features. The manufacturing skill is realistic and lively [78]. The painted sculptures in the Chongqing Temple are the outstanding representative in the Song Dynasty (Fig. 19b). Its moulding sequence is wood skeleton→ straw rope→ coarse clay layer→ fine clay layer→ pigment layer (including plaster). The painted sculptures had no limb defects and wooden skeleton was intact. It showed that when selecting materials and building the skeleton, the craftsmen spent much thought and effort. The fine clay layer was mixed with cotton and hemp fibers, and its thickness was 2–4 mm, which was thinner and more refined than other dynasties. The soil of the base layer contained illite 18%–28%, quartz 26%–36% [80], which made the soil have the characteristics of low hygroscopicity, low shrink-swell properties, and strong weathering resistance.

The Yuan Dynasty

The style characteristic of the painted sculptures in the Yuan Dynasty is to express the image and emotion of the statue. The craftsmen broke away from the bondage of break the religion, and integrated into their subjective view. The painted sculptures during this period appeared the trend of secularize [81]. The Twenty-Eight Mansions painted sculptures in the Jade Emperor Temple are rare in China's traditional sculptures of Taoist (Fig. 19d). The moulding sequence is wood skeleton→ straw rope→ coarse clay layer→ fine clay layer→ hemp paper→ pigment layer [82]. The researchers found that the craftsmen used hemp paper instead of plaster. This step is different from previous dynasties. The hemp paper is helpful to block and cover the propagation of cracks. The main mineral composition of the base layer was kaolinite, which was the best clay to make sculptures [83].

The Ming and the Qing Dynasty

The painted sculptures in the Ming and Qing Dynasty imitated the Tang Dynasty in art style, but the charm and momentum was inferior to the Tang Dynasty [78]. Shuilu'an Temple is famous for its delicately painted sculptures of Ming Dynasty (Fig. 19e). The technique of making sculptures is wood skeleton→ coarse clay layer→ fine clay layer→pigment layer (including plaster) [84]. The painted sculptures in the Houtu Temple were built in the Qing Dynasty (Fig. 19f). The researchers found some samples of the painted sculptures in the Houtu Temple did not have the fine clay layer [85]. It proved that the craftsmanship of the painted sculptures in the Qing Dynasty was no more elaborate. Compared with the craftsmanship of previous dynasties, it is easy to find the manufacturing processes tend to simplify. This is because rulers' dependence on religion is declining.

Development of Chinese painted sculptures craftsmanship

In the above, we summarized how several representative dynasties made painted sculptures. It can be seen that the development of painted sculptures is inextricably linked to the comprehensive national power, national customs, and ruler's respect for religion. The Liao and Song dynasties are in the same historical period, but the craftsmanship and style of painted sculptures have their own characters. It shows that history and national culture have a great influence on the manufacturing of painted sculptures. In short, the manufacturing process of painted sculptures is basically normative, but the specific details are different.

Conclusions

Based on the analysis of the internal structure and pigment layer, the craftsmanship and the materials of the painted sculptures are basically clear. The following conclusions are obtained.

As for the craftsmanship, this paper summarized the moulding sequence of the painted Bodhisattvas sculptures in the Fengguo Temple. The skeleton structure of the Bodhisattvas is unequivocal. The main skeletons of the upper body are irregular frame structures connected by wooden boards and metal connectors. For the lower structure, it can be basically divided into two types, i.e. with a penetrative pillar or not.

In regard to the materials, the mineral composition of the pigments is determined by various analysis methods. The results show that the red pigment is the combination of cinnabar and minium, while the

green and blue pigment is atacamite and Prussian blue, respectively. The coarse clay layer is reinforced with wheat straw and the fine clay layer with hemp, which can increase the tensile strength of the soil effectively and improves the shrinkage of the soil. Sand is added to the fine clay layer as well to increase its strength and weathering resistance.

According to the analysis of the craftsmanship and materials of the painted Bodhisattva sculptures in the Fengguo Temple, we not only understand the construction methods and material characteristics of the sculptures in the Liao Dynasty, but also lay a solid foundation for the follow-up conservation and restoration. The subsequent study on the Bodhisattva should focus on the deterioration mechanism, repair materials, environmental temperature and humidity regulation, regular cleaning and other aspects. It is crucial to form a complete and practical protection and repair program.

In the second half of this article, we outlined the development of Chinese painted sculptures craftsmanship. We selected a few typical examples to show the special features of painted sculpture manufacturing process in different dynasties. The national power, folk customs, and beliefs of a dynasty will have an impact on the artistic style of painted sculptures. Deducing the history and culture of a dynasty by studying the craftsmanship of painted sculptures is also an interesting and meaningful subject.

Our study in this paper provides references for the study of the craftsmanship and materials of these statues, as well as the research methods and ideas. Due to the long history of China, there remain many precious and exquisite painted sculptures in temples or grottoes. They deserve in-depth study and explore.

Acknowledgements
The authors are grateful to researchers Ke Bai, Yan Yan for their hard on-the-spot investigation. Researchers Xiaojuan Dang, Yongjin Wang, Jiankai Xiang, Shaohua Dong are gratefully acknowledged for their contribution of X-ray photos shooting and experimental analysis. All the researchers above are from Shaanxi Institute for the Preservation of Cultural Heritage. Thanks are due to Shengfeng Institute of Novel Geological Techniques Ltd. Xinjiang Branch, for the analysis of ground-penetrating radar. Thanks to associate professor Ni Xie for the revision and guidance of the article structure and language. We are finally much obliged to the Heritage Management Office of Yi County, for the hospitality extended to us during our stay at site and assistance provided throughout the project.

Authors' contributions
JHS wrote most of the initial versions of the text. SJY and WX revised the manuscript critically for important intellectual content. LYM and WQZ provided and analyzed the data. All authors contributed to research strategy, the discussion and interpretation of the results and to the final form of the text and figures. All authors read and approved the final manuscript.

Funding
The research is financially supported by National Natural Science Foundation of China (Grant No. 41672297).

Availability of data and materials
The data sets analyzed during the current study are available from the corresponding author on reasonable request.

Competing interests
All authors declare that they have no competing interest.

Author details
[1] Faculty of Engineering, China University of Geosciences (Wuhan), Hongshan District, Lumo Road, No 388, Wuhan 430074, China. [2] School of Cultural Heritage, Northwest University, Yanta District, Taibai Road No 229, Xi'an 710069, China. [3] Shaanxi Institute For The Preservation of Cultural Heritage, Hi-tech District, Keji 1st Road, No 35, Xi'an 710075, China.

Received: 12 October 2020 Revised: 15 January 2021 Accepted: 18 January 2021
Published online: 28 January 2021

References

1. Tentative Lists UNESCO. 2014. http://whc.unesco.org/en/tentativelists/5803/. Accessed 4 May 2019.
2. Sekino T. The Main Shrine Hall of the Fengguo Temple in Yixian, Manchuria. Art Studies. 1933;14:1–12.
3. Du XZ. Investigation of the Great Hall of Fengguo Temple in Yi County. Cultural Relics. 1961;2:5–13. **(in Chinese)**.
4. Steinhardt NS. Liao: an architectural tradition in the making. Artibus Asiae. 1994;54(1/2):5–39.
5. Bai CJ. Research on application of laser 3D scanning technology in ancient architecture measuring & relative issues. Master's thesis. Tianjin University, Tianjin. 2007.
6. Wei R, Liu C. Investigation and analysis of soluble salts in mural paintings of Fengguo Temple in Liaoning Province. Identification Appreciation Cultural Relics. 2018;13:92–3 in chinese.
7. Lluveras-Tenorio A, Bonaduce I, Sabatini F, et al. The organic materials in the five Northern Provinces' Assembly Hall: disclosing the painting technique of the Qing dynasty painters in civil buildings. Appl Phys A Mater. 2015;121(3):879–89.
8. Gill MS, Rendo CP, Menon S. Materials and techniques: early Buddhist wall paintings and sculptures at Sumda Chun. Ladakh Stud Conserv. 2014;59(5):300–13.
9. Wei JW. Non-destructive testing and evaluation on ancient Chinese colored-clay sculptures. Int Conf Electr Technol Civ Eng ICETCE Proc. 2011; 3271–6.
10. Liu RZ, Zhang BJ, Zhang H, Shi MF. Deterioration of Yungang Grottoes: diagnosis and research. J Cult Herit. 2011;12(4):494–9.
11. Gettens RJ. The freer Chinese bronzes, volume II, technical studies. Oriental studies. 1969; 7.
12. Takayasu K. An introduction to the conservation science of archaeological relics. Nara: National Research Institute for Cultural Properties; 2004. p. 18.
13. Tian XL, Zhou X, Gao F. Nondestructive testing and analysis technology in the field of heritage preservation. Nondestructive testing. 2008;30(3):178–82.
14. Zhou H, Yang M, Gao F, et al. Application of portable X-ray radiography to assess the weathering condition of the Avalokitesvara Sculpture in Dazu Rock Carvings. Sci Conserv Archaeol. 2012;24(4):45–54. **(in Chinese)**.
15. Mannes D, Benoît C, Heinzelmann D, et al. Beyond the visible: combined neutron and X-ray imaging of an altar stone from the former Augustinian church in Fribourg, Switzerland. Archaeometry. 2014;56(5):717–27.
16. Vaughan CJ. Ground-penetrating radar surveys used in archaeological investigations. Geophysics. 1986;51(3):595–604.
17. Tsokas GN, Giannopoulos A, Tsourlos P, et al. A large scale geophysical survey in the archaeological site of Europos (northern Greece). J Appl Geophys. 1994;32(1):85–98.
18. Berard BA, Maillol JM. Multi-offset ground penetrating radar data for improved imaging in areas of lateral complexity—application at a Native American site. J Appl Geophys. 2007;62(2):167–77.

19. Yalçiner C, Bano M, Kadioglu M, et al. New temple discovery at the archaeological site of Nysa (western Turkey) using GPR method. J Archaeol Sci. 2009;36(8):1680–9.
20. Huang LX, Gao PF, Xiao GQ. Experiment of probing thickness of the Mogao Grottoes Frescoes by the ground penetrating radar. J Liaoning Technical University (Nat Sci). 2001;20(4):457–9 (in Chinese).
21. Mizusawa K. Polarizing microscope observations of pottery from the Yashiro sites, Nagano Prefecture, Central Japan. Quat Int. 2016;397:495–503.
22. Xia Y, Xi N, Huang J, et al. Smalt: an under-recognized pigment commonly used in historical period China. J Archaeol Sci. 2019;101:89–98.
23. Nerantzis N, Bassiakos Y, Papadopoulos S. Copper metallurgy of the Early Bronze Age in Thassos, north Aegean. J Archaeol Sci: Rep. 2016;7:574–80.
24. Zhao YX, Bing Y, Zhao BD, et al. Evolutions of aperture gaps and grain sizes in surface layers of Southern Xiangtang Carvings and related environmental pollutions. J Jilin Univ. 2006;36(3):133–8.
25. Favaro M, Vigato PA, Andreotti A, et al. La Medusa by Caravaggio: characterisation of the painting technique and evaluation of the state of conservation. J Cult Herit. 2005;6(4):295–305.
26. Doménech-Carbó A, Doménech-Carbó MT, Moya-Moreno M, et al. Identification of inorganic pigments from paintings and polychromed sculptures immobilized into polymer film electrodes by stripping differential pulse voltammetry. Anal Chim Acta. 2000;407(1–2):275–89.
27. Wang R, Nie F, Chen JM, et al. Studies on lacquerwares from between the Mid-Warring States Period and the Mid-Western Han dynasty excavated in the Changsha region. Archaeometry. 2017;59(3):547–65.
28. Wei G, Zhang H, Wang H, et al. An experimental study on application of sticky rice–lime mortar in conservation of the stone tower in the Xiangji Temple. Constr Build Mater. 2012;28(1):624–32.
29. Schreiner M, Melcher M, Uhlir K. Scanning electron microscopy and energy dispersive analysis: applications in the field of cultural heritage. Anal Bioanal Chem. 2007;387(3):737–47.
30. Wang W, Zhu J, Jiang J, et al. Microscopic analysis of "iron spot" on blue-and-white porcelain from Jingdezhen imperial kiln in early Ming dynasty (14th–15th century). Microsc Res Tech. 2016;79(11):1123–30.
31. Harbottle G. The Vinland Map: a critical review of archaeometric research on its authenticity. Archaeometry. 2008;50(1):177–89.
32. Čechák T, Trojek T, Musílek L, et al. Application of X-ray fluorescence in investigations of Bohemian historical manuscripts. Appl Radiat Isot. 2010;68(4–5):875–8.
33. Kim M, Lee J, Doh JM, et al. Characterization of ancient Korean pigments by surface analytical techniques. Surf Interface Anal. 2016;48(7):409–14.
34. Wang L, Yang L, Zhou W, et al. Analysis of the techniques and materials of the coloured paintings in the Renshou Hall in the Summer Palace. Anal Methods-UK. 2015;7(12):5334–7.
35. Zhu J, Duan H, Yang Y, et al. Colouration mechanism of underglaze copper-red decoration porcelain (AD 13th–14th century), China. J Synchrotrons Radiat. 2014;21(4):751–5.
36. Kriznar A, Muñoz MV, de la Paz F, et al. Non-destructive XRF analysis of selected Flemish panel paintings in the Fine Arts Museum of Seville. J Inst Conserv. 2014;37(2):136–51.
37. Daniilia S, Sotiropoulou S, Bikiaris D, et al. Panselinos' Byzantine wall paintings in the Protaton Church, Mount Athos, Greece: a technical examination. J Cult Herit. 2000;1(2):91–110.
38. Ingo GM, Balbi S, De Caro T, et al. Combined use of SEM-EDS, OM and XRD for the characterization of corrosion products grown on silver roman coins. Appl Phys A-Mater. 2006;83(4):493–7.
39. Marszałek M. Identification of secondary salts and their sources in deteriorated stone monuments using micro-Raman spectroscopy, SEM-EDS and XRD. J Raman Spectrosc. 2016;47(12):1473–85.
40. Bonaduce I, Blaensdorf C, Dietemann P, et al. The binding media of the polychromy of Qin Shihuang's Terracotta Army. J Cult Herit. 2008;9(1):103–8.
41. Bowitz J, Ehling A. Non-destructive infrared analyses: a method for provenance analyses of sandstones. Environ Geol. 2008;56(3–4):623–30.
42. Yao D, Li C. Investigation Report of the Daxiong Hall of Fengguo Temple at Yixian in Liaoning Province. Architectural History. 2009;25:10–33. **(in Chinese)**.
43. Lehmann EH, Vontobel P, Deschler-Erb E, et al. Non-invasive studies of objects from cultural heritage. Nucl Instrum Meth A. 2005;542(1–3):68–75.
44. Harry MJ. Ground penetrating radar: theory and applications. Oxford: Elsevier Science; 2009.
45. Lawrence BC. Ground-penetrating radar for geoarchaeology. New Jersey: Wiley; 2016.
46. Marel HW Van der, Beutelspacher H. Atlas of infrared spectroscopy of clay minerals and their admixtures. Amsterdam: Elsevier; 1976.
47. Hu K, Bai C, Ma L, et al. A study on the painting techniques and materials of the murals in the Five Northern Provinces' Assembly Hall, Ziyang, China. Herit Sci. 2013;1(1):18.
48. Ji J, Zhang JF. The origin and history of some blue pigments in ancient China. Dunhuang Res. 2011;6:109–14 (in Chinese).
49. Barbara HS. Infrared spectroscopy: fundamentals and applications. New Jersey: Wiley; 2005.
50. Michele RD, Dusan S, James ML. Infrared spectroscopy in conservation science. Los Angeles: Getty Conservation Institute; 1999.
51. Dong SH, Yang JC, Shu JP, et al. Rapid identification of powdery rust using transmission infrared microspectroscopy. Sci Conserv Archaeol. 2019;31(1):113–9. **(in Chinese)**.
52. Wang JY, Wang JC. Textual research of copper green in ancient China. National Academic Conference on Archaeology and Cultural Relics Protection. 2007 (**in Chinese**).
53. MacEwan DMC, Wilson MJ, Brindley GW, et al. Interlayer and intercalation complexes of clay minerals. Crys Struct Clay Minerals Their X-ray Identification. 1980;5:197–248.
54. Yang QY. Discussion on the research system of traditional techniques of color-painted clay sculptures in ancient temples. Relics Museol. 2015;4:48–55 (in Chinese).
55. Wang N, He L, Egel E, et al. Complementary analytical methods in identifying gilding and painting techniques of ancient clay-based polychromic sculptures. Microchem J. 2014;114:125–40.
56. Dickson FW, Tunell G. The stability relations of cinnabar and metacinnabar. Am Mineral. 1959;44(5–6):471–87.
57. Thieme C. Paint layers and pigments on the terracotta army: a comparison with other cultures of antiquity. Monuments Sites. 2001;3:52–8.
58. Wang JY, Wang JC. Application of vermilion pigments in ancient China. Sci Conserv Archaeol. 1999;11(1):40–5. **(in Chinese)**.
59. Wang N, Zhang T, Min J, et al. Analytical investigation into materials and technique: carved lacquer decorated panel from Fuwangge in the Forbidden City of Qianlong Period, Qing Dynasty. J Archaeol Sci: Rep. 2018;17:529–37.
60. Edwards HGM, Farwell DW, Rozenberg S. Raman spectroscopic study of red pigment and fresco fragments from King Herod's Palace at Jericho. J Raman Spectrosc. 1999;30(5):361–6.
61. Daniilia S, Minopoulou E. A study of smalt and red lead discolouration in Antiphonitis wall paintings in Cyprus. Appl Phys A Mater. 2009;96(3):701–11.
62. Sakr AA, Ghaly MF, Geight ESF, et al. Characterization of grounds, pigments, binding media, and varnish coating of the Angel Michael' icon, 18th century, Egypt. J. Archaeol. Sci: Rep. 2016; 9: 347 – 57.
63. Demir S, Şerifaki K, Böke H. Execution technique and pigment characteristics of Byzantine wall paintings of Anaia church in Western Anatolia. J Archaeol Sci: Rep. 2018;17:39–46.
64. Zhang Y, Wang J, Liu H, et al. Integrated analysis of pigments on murals and sculptures in Mogao Grottoes. Anal Lett. 2015;48(15):2400–13.
65. Su BM, Hu ZD, Li ZX. A study of the mixed pigments used in the wall paintings of Dunhuang. Dunhuang Res. 1996;3:149–62 (in Chinese).
66. Giovannoni S, Matteini M, Moles A. Studies and developments concerning the problem of altered lead pigments in wall painting. Stud Conserv. 1990;35(1):21–5.
67. Mike W. Prussian blue: artists' pigment and chemists' sponge. J Chem Educ. 2008;85(5):612.
68. Berger JE. (ca. 1730) Kernn aller Fridrichs-Städtischen Begebenheiten. handwritten manuscript, Berliner Staatsbibliothek Preussischer Kulturbesitz, Ms. Bor Quart. 124, p. 26.
69. Bartoll J. The early use of Prussian blue in paintings. Proceedings of the 9th International Conference on NDT of Art. 2008.
70. Bailey K. A note on Prussian blue in nineteenth-century Canton. Stud Conserv. 2012;57(2):116–21.
71. Yang B, Li GH, Qu L, et al. Preliminary scientific analysis of colored reverse painting on glass in Qing Dynasty. Chin Cult Relics Res. 2017;3:74–81 (in Chinese).

72. Newman ACD. Chemistry of clays and clay minerals. Longman Scientific & Technical. 1987, 480.
73. Li T. Pigment and fiber use in ancient Chinese paper currencies and pawn ticket. China Numismatics. 2018;1:8–17. **(in Chinese)**.
74. Duan XY. Knowledge of the making materials of the murals in Mogao Grottoes. Dunhuang Res. 1988;3:46-64 + 122-3 (in Chinese).
75. Juan F. The study on the properties and repair materials of the soil of clay sculptures in the Shuilu'an Temple. Archaeol Cult Relics. 1994;6:30–41 (in Chinese).
76. Rickerby S, Shekede L, Fan Z, et al. Development and testing of the grouting and soluble-salts reduction treatments of cave 85 wall paintings. Conserv Ancient Sites Silk Road. 2010; 471–9.
77. Yang JF. A study of the national style of Buddhist statues in Liao Dynasty. Art Panorama. 2019;8:71. – 3. **(in Chinese)**.
78. Cheng DS. The painted sculptures in Shanxi Province. Traditional Chin Architect Gardens. 2001;4:10–7 (in Chinese).
79. Xu N. The preliminary study of manufacturing technology analysis and virtual restoration of clay sculptures in the Qinglian Temple, Jincheng, Shanxi. Master's thesis. Northwest University, Xi'an. 2014.
80. Yu QL, Yan M, Yang QY. Disease investigation and analysis of the color modeling from Song Dynasty of Chongqing Temple. Relics Museol. 2009;6:280–4 (in Chinese).
81. Zhang RC. The study of the Yuan Dynasty painted sculptures in the Main Hall of the Guangji Temple. Master's thesis. Taiyuan University of Technology, Taiyuan. 2019.
82. Yang QY. Analysis on the Characteristics of Ancient Painted Clay Sculptures in Southeastern Shanxi. China Heritage News. 2007.11.28.
83. Liu LX. A preliminary study on the restoration of the painted process of the painted clay sculptures in the Jade Emperor Temple in Jin City, Shanxi Province. Relics Museol. 2014;5:94–6 (in Chinese).
84. Gao Y. Study about the conservation and restoration of wall-modeling sculptures and hanging sculptures in Shuilu'an Temple. Master's thesis. Northwest University, Xi'an. 2015.
85. Li YF. A research on the conservation of color-painted sculptures of Houtu Temple in Jiexiu Shanxi Province. Master's thesis. Lanzhou University, Lanzhou. 2007.

Publisher's note